

Supplemental Information

Cold denaturation of DNA origami nanostructures

Daniel Dornbusch,^{a,c} Marcel Hanke,^b Emilia Tomm,^b Charlotte Kielar,^{a,d} Guido Grundmeier,^b Adrian Keller,^{*b} and Karim Fahmy^{*a,c}

^a Helmholtz-Zentrum Dresden-Rossendorf, Institute of Resource Ecology, Bautzner Landstrasse 400, 01328 Dresden, Germany. Email: k.fahmy@hzdr.de

^b Paderborn University, Technical and Macromolecular Chemistry, Warburger Str. 100, 33098 Paderborn, Germany. E-mail: adrian.keller@uni-paderborn.de.

^c Technische Universität Dresden, BIOTEC, Cluster of Excellence Physics of Life, Dresden 01062, Germany.

^d Helmholtz-Zentrum Dresden-Rossendorf, Institute of Ion Beam Physics and Materials Research, Bautzner Landstrasse 400, 01328 Dresden, Germany.

*Corresponding authors

1. DNA origami synthesis

DNA origami triangles¹ in 100 μL were prepared by combining the following three solutions: 30 μL scaffold p7249 (M13mp18 plasmid), 100 nM, from Tilibit), 60 μL staple strands (500 nM, from Eurofins) and 10 μL of Tris/MgAc₂ buffer (100 mM). The mixture was subjected to temperature ramping using the Primus 25 advanced Thermocycler (PEQLAB, Erlangen, Germany). The temperature was gradually decreased from 80°C to room temperature (RT) over a period of 90 minutes. The concentration of DNA origami nanostructures was determined using an Implen Nanophotometer P330 (Implen GmbH, Munich).

Spin filtration was used to purify the DNA origami. 200 μL of origami solution and 200 μL of 10 mM Tris+Mg buffer were added to an Amicon Ultra-0.5 centrifugal filter (Merck). The mixture was centrifuged at 6000 rpm for 10 minutes. The 'wash' solution was discarded and 300 μL of 10 mM Tris/MgAc₂ buffer was added to the filter. The centrifugation was repeated for another 10 min. Finally, the filter was inverted, placed in a new tube and centrifuged at 7000 rpm for 10 minutes. If necessary, the concentration was re-adjusted to 100 nM using 10 mM Tris/MgAc₂ buffer.

2. AFM imaging

An 8 M solution of GdmCl was purchased from Sigma Aldrich. For each experiment, a 100 μL solution consisting of 5 nM DNA origami triangles, 4 M GdmCl and 10 mM TRIS buffer with 10 mM MgAc₂ was prepared in a PCR tube and incubated in a Primus25 advanced Thermocycler at 5, 10 and 20 °C for 60 min, respectively. Subsequently, 1 μL of the solution was deposited on a freshly cleaved mica surface and immediately covered with 100 μL of the buffer solution. After 5 min of incubation, the mica sample was washed with about 10 mL HPLC-grade water (VWR) and dried under a stream of Ar. AFM imaging was performed in PeakForce Tapping ScanAsyst mode using a Bruker Dimension ICON with an image size of 3 x 3 μm^2 and 1024 x 1024 px at 1 Hz scan rate.

3. Liquid AFM Imaging of “cut triangles”

DNA origami triangles with a “cut” into one of the trapezoids were prepared as above with the exclusion of five staple strands (Table S1) and diluted to 5 nM with HPLC-grade water (VWR). For the measurement in liquid, the samples were incubated in a Mastercycler personal Thermocycler (Eppendorf, Hamburg, Germany) at 5 °C and 20 °C for 60 min as described in chapter 2. The 5 °C sample was then transferred to the AFM in an ice bath. Basically, the sample preparation was carried out as described in chapter 2. For the AFM measurement in liquid, 5 µl of the Origami solution was deposited on mica and covered with 100 µl of the buffer solution. After an incubation time of 5 min, the sample was washed with 3 mL HPLC grade water (VWR) and filled up with 100 µl HPLC grade water for the liquid measurement. The AFM imaging was performed with a Cypher ES (Asylum Research, Goleta, CA, USA). The liquid samples were measured in tapping mode with a Biolever Mini BL-AC40TS-C2 cantilever (Olympus, Tokyo, Japan) and with temperature-controlled chamber at 5 °C, 20 °C and room temperature (RT). The images were recorded with a scan size of 3 x 3 µm², 1.5 x 1.5 µm² and 0.6 x 0.6 µm², a line rate of 1 Hz and 1024 x 1024 px or 512 x 512 px.

Table S1: Shows the non-inserted oligonucleotide sequences of the Rothmund triangle origami.¹

staple strand	oligonucleotide sequence
t-1s26i	CTCTAGAGCAAGCTTGCATGCCTGGTCAGTTG
t-1s28i	CCTTCACCGTGAGACGGGCAACAGCAGTCACA
t-1s30e	CGAGAAAGGAAGGGAAGCGTACTATGGTTGCT
t1s26i	GCAAATCACCTCAATCAATATCTGCAGGTCGA
t1s28i	CGACCAGTACATTGGCAGATTCACCTGATTGC

4. CD spectroscopy and principal component analysis

DNA origami solutions (60 μL , approximately 100 nM) were mixed with GdmCl salt stock solutions and Tris/MgAc₂ buffer to a total of 150 μL at a final concentration of 40 to 45 nM DNA origami triangles in 10 mM Tris, 10 mM MgAc₂ and 4 M GdmCl buffer. The concentration of DNA origami was calculated from the absorbance at 260 nm at 20 °C using an extinction coefficient of 0.0263 ($\mu\text{g}/\text{ml}$)⁻¹ cm⁻¹ and a molecular weight of 4472.760 kg/mol, according to the size and GC content of the M13mp18 DNA. Spectroscopic measurements were performed in a 1 mm quartz cuvette (Helma) using a Jasco 815 CD spectrometer with a cold denaturation protocol decreasing the temperature from 37 °C to 1 °C at a cooling rate of 0.5 °C/min. Spectra were recorded from 315 nm to 215 nm with a data pitch of 1 nm, a scan speed of 50 nm/min, a bandwidth of 3 nm and a digital integration time (D.I.T.) of 2 seconds. The threshold for the spectroscopic data was set at a high voltage of 600 V.

Abstract principal components in the temperature dependence of the measured CD spectra were determined by the iterated target function analysis (ITFA) program.² First, we analyzed the eigenvalues of the covalent data matrix and the given relative uncertainties from the PCA. The Varimax rotation was then performed for two and three components, which allows coordinate systems to be rotated in n-dimensional spaces to identify the temperature dependence of the most prominent spectral changes (Fig. S1).³ However, an assignment of the corresponding component spectra to DNA structural features is speculative and was not attempted here.

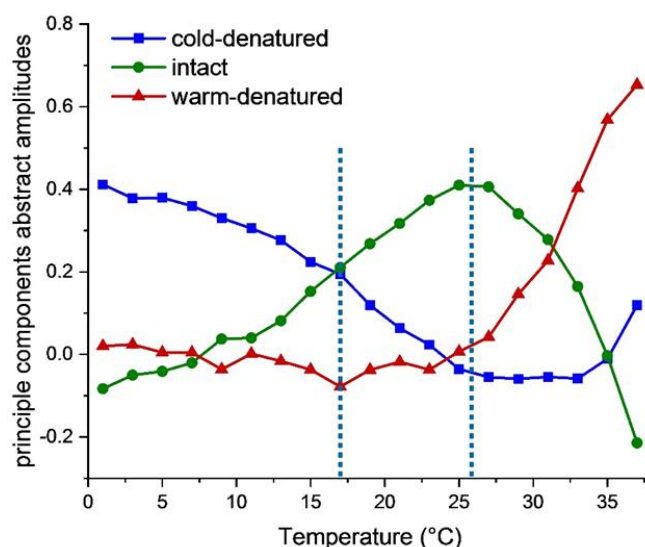


Figure S1: Varimax result of fitting temperature-dependent CD spectra of normal DNA origami triangles in 4M GdmCl by three principle components. The traces reproduce the salient feature of the two-component analysis with 50 % cold-denaturation occurring at 17 °C and a maximal population of intact DNA origami at 26 °C. The main difference with respect to the two-component fit is the rise of a third warm denatured state (red). It is spectroscopically very similar to the cold denatured state and is not due to global melting (which has a T_m between 50 and 60 °C). Due to this similarity, the rise of third component can largely make up for the smaller amplitude of the cold-denatured state above 26 °C. In fact, the occurrence of a negative amplitude is indicative of mutually compensating effects in the three-component fit, showing that two components already pick up the salient features of the temperature-sensitive spectral changes.

5. Additional AFM images

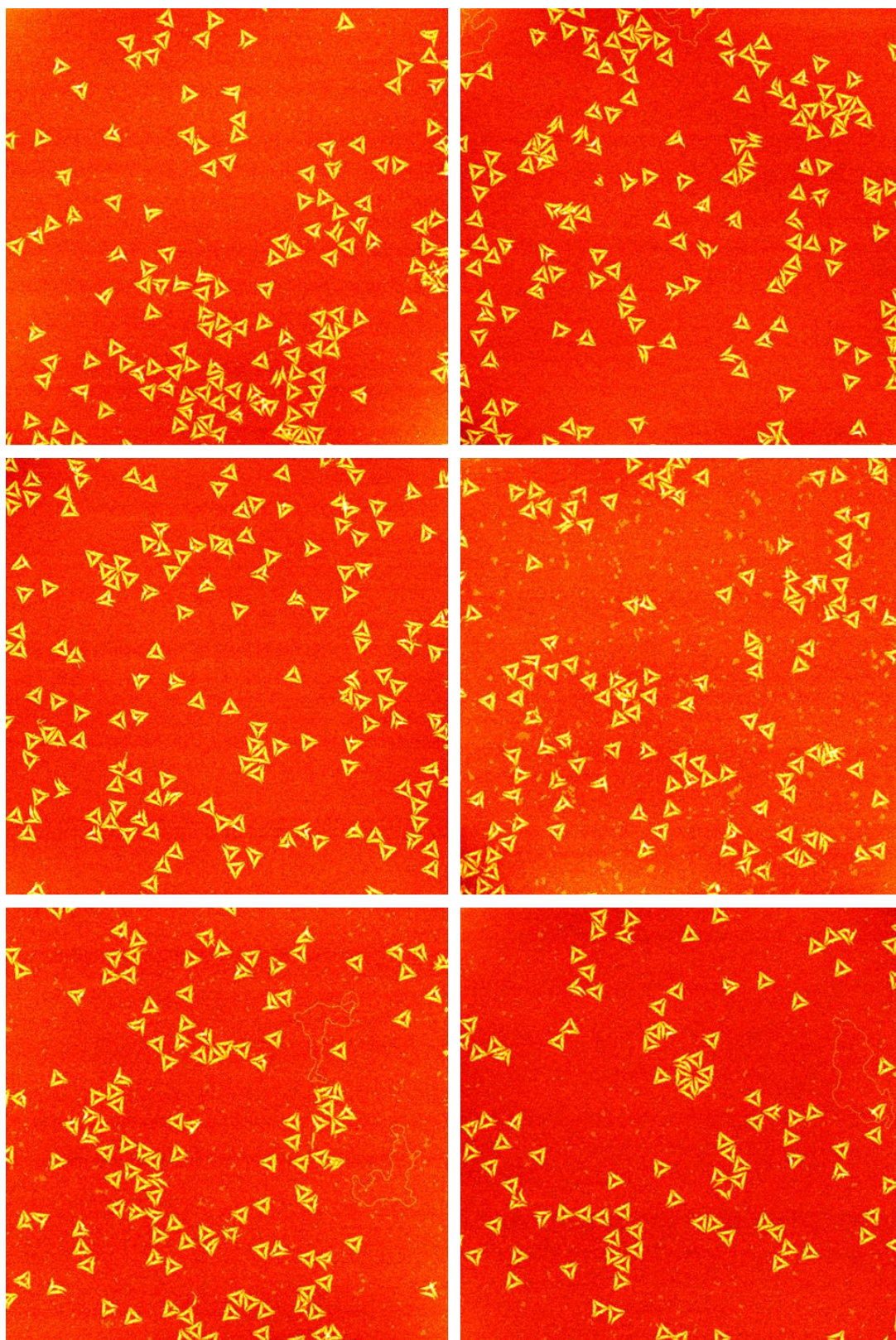


Figure S2: Additional AFM images ($3 \times 3 \mu\text{m}^2$) of DNA origami triangles after incubation at 5°C . Height scales are 3.0 nm.

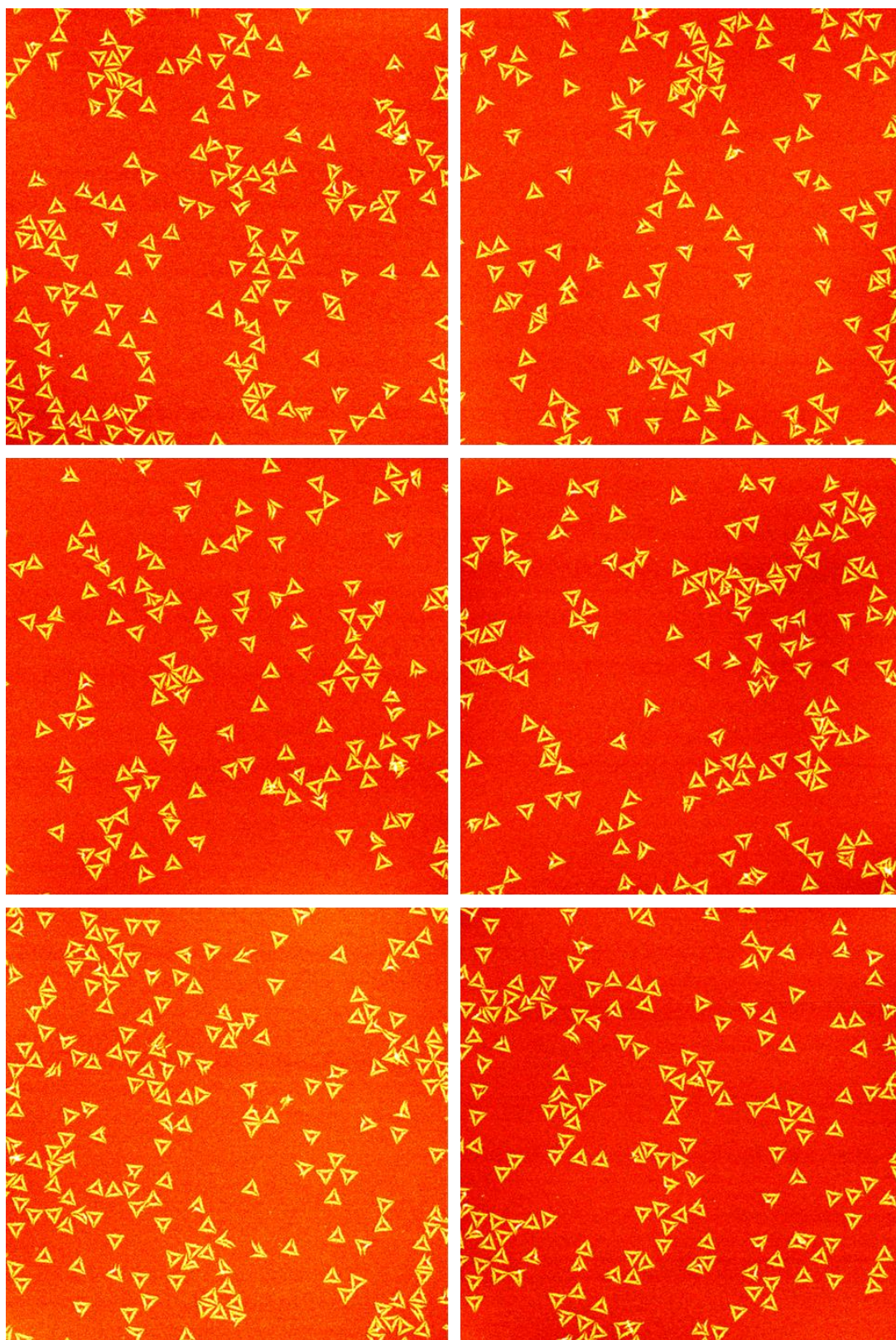


Figure S3: Additional AFM images ($3 \times 3 \mu\text{m}^2$) of DNA origami triangles after incubation at 10°C . Height scales are 3.0 nm.

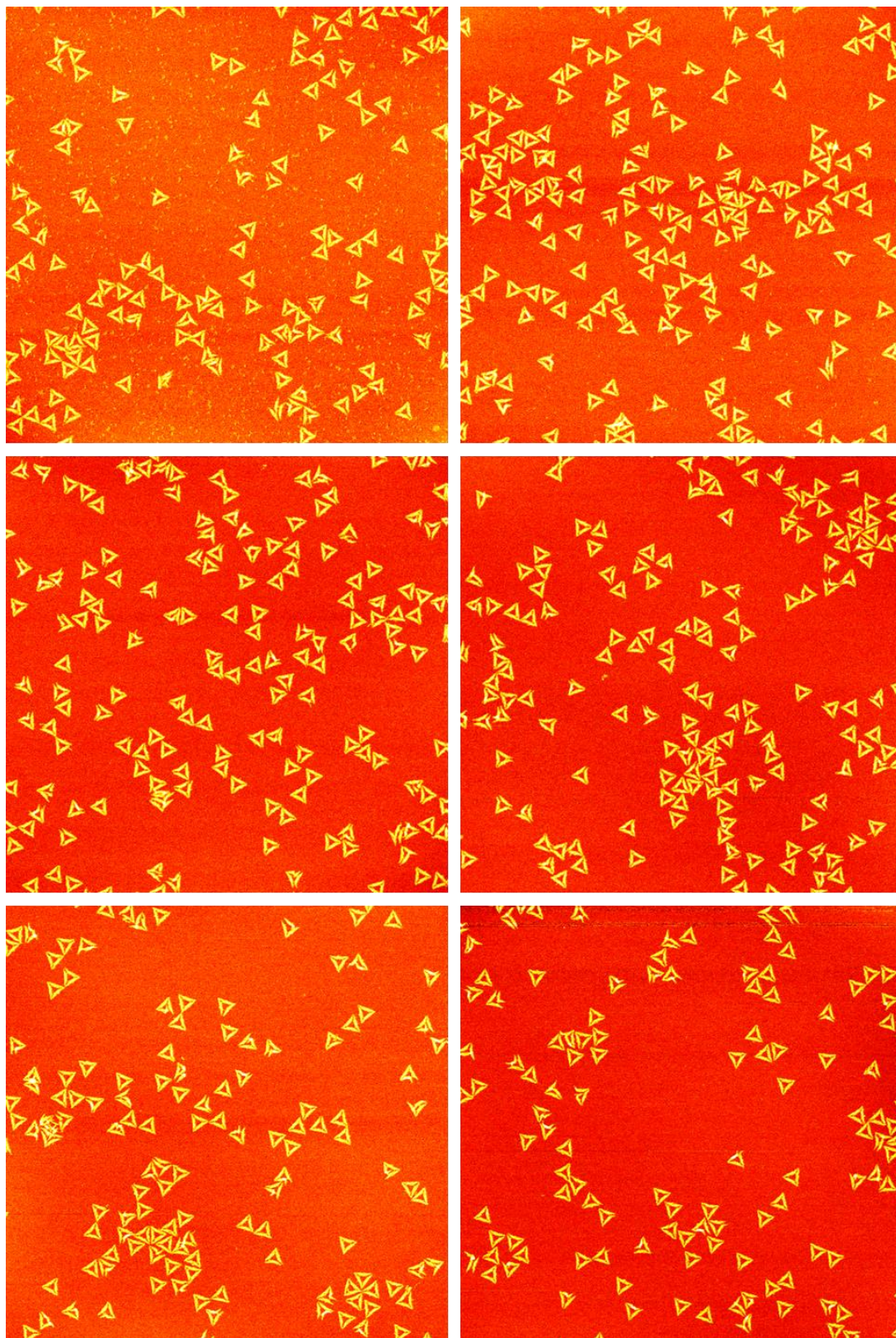


Figure S4: Additional AFM images ($3 \times 3 \mu\text{m}^2$) of DNA origami triangles after incubation at 20°C . Height scales are 3.0 nm.

6. Cold-denaturation of the vertices is suppressed by reduced strain in the trapezoids

We have designed “cut triangles”, i.e., DNA origami triangles in which five out of nine connecting staples at the center of one of the trapezoids were removed (staple designations: t-1s26i, t1s26i, t-1s28i, t1s28i, t-1s30e) leading to a visible “cut” into the trapezoid as shown in Fig. S5. Thereby, we disrupted the connectivity which transmits strain within the supramolecular assembly between distant structural elements. The removal of the five staple strands concerns only 1,1 % of the total amount of bases in the DNA origami but causes much larger intensity changes in the CD spectra shown in Fig. S6. This confirms that a global structural effect is exerted on the triangular nanostructures by the local destabilization of only one trapezoid which reduces suprastructural strain transmitted along the architectural elements.

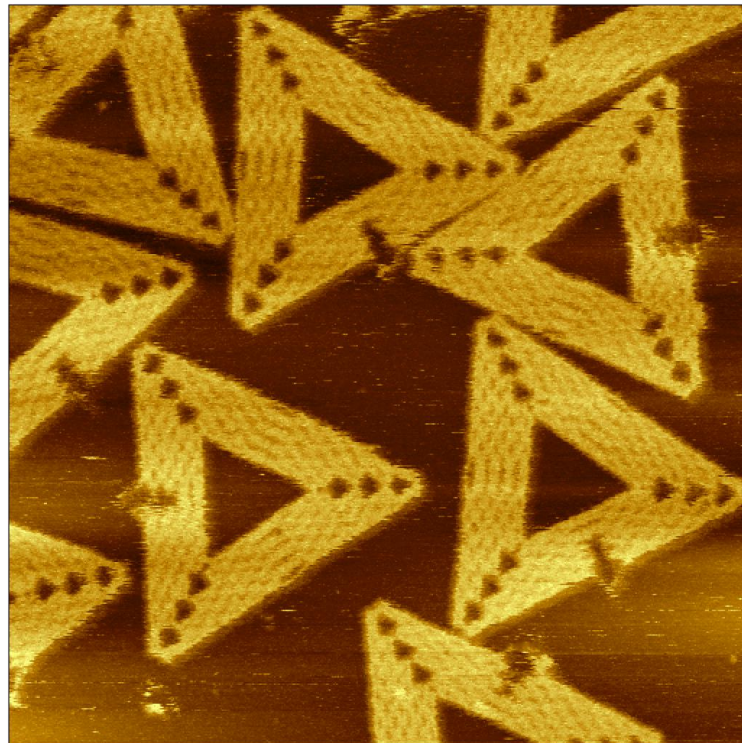


Figure S5: Detail AFM image ($0.3 \times 0.3 \mu\text{m}^2$) of “cut triangles”, i.e., DNA origami triangles which lack 5 staple strands, after incubation at RT without GdmCl, measured in liquid. Height scales are 5.0 nm.

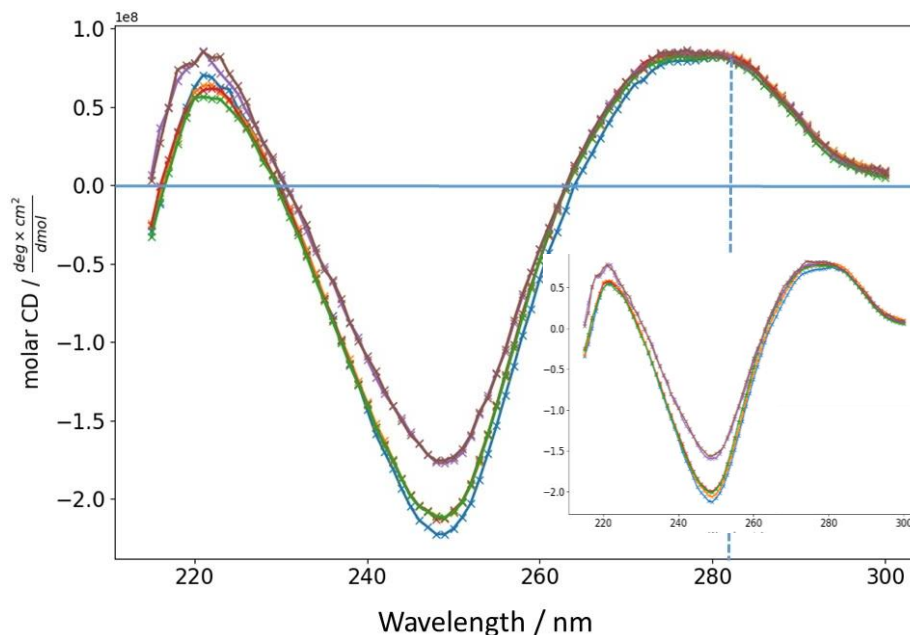


Figure S6: CD spectra of “cut triangles” (brown and violet traces) at 5 °C compared with normal triangles (red, orange, green, blue traces). Spectra are normalized to the 282 nm intensity, thereby, emphasizing the large difference in the positive lobe relative to the negative lobe in the CD spectra of the two DNA origami designs. Violet and brown traces are spectra from “cut triangles” measured at 5 °C or measured after a second cooling to 1 °C after warming to 37 °C, respectively. The virtual identity of the spectra after two temperature scans evidences the reversibility of temperature-induced structural changes. Blue and orange traces are from two independent measurements of normal triangles. Red and green traces have been recorded after a first and a second cooling to 1 °C, respectively. Inset: CD spectra of the same samples at 21 °C (same colour-coding). All samples were in 4 M GdmCl.

At 21 °C, the negative amplitude in the spectra of “cut triangles” became slightly reduced, evidencing that the structure undergoes thermal transitions. These transitions are most likely related to the collapse of the cut trapezoids which increased with temperature (Fig. S7), rather than being a cold-induced damage. Remarkably, the fractions of broken “cut triangles” and dissociated vertices did not show any temperature sensitivity (Fig. S7). Furthermore, the fraction of dissociated vertices was by two thirds smaller than in normal DNA origami triangles, in agreement with the notion that the cut in the trapezoids prevented transmission of strain to the vertices.

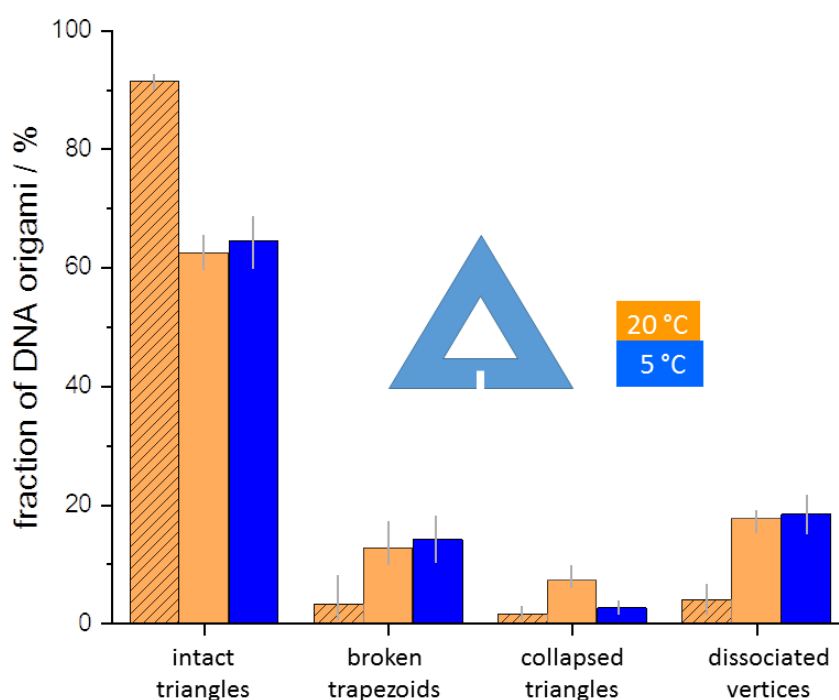


Figure S7: Fractions of intact “cut triangles” and of types of damage as a function of temperature. Reference data taken at room temperature (RT) in 10 μ M Tris/MgAc₂ buffer in the absence of GdmCl are hatched, otherwise the data were obtained from samples with 4 M GdmCl in Tris/MgAc₂ buffer, error bars in gray. In contrast to normal DNA origami triangles, none of the statistically evaluated damage fractions increased upon cooling. The evaluated data are given in Table S2.

The most appropriate control for maximal release of supramolecular strain in the fully base-paired scaffold is the dsDNA of the M13mp18 plasmid itself. CD spectra of the dsDNA plasmid in 4 M GdmCl show virtually no differences between 1 °C and 37 °C (Fig. S8) and lack the typical 282 nm CD band of DNA origami triangles in GdmCl. Since the base composition of dsDNA of M13mp18 is the same, it is the supramolecular arrangement in the normal DNA origami triangles that causes the cold-induced build-up of strain leading to both, the change of chirality at 282 nm and the dissociation of the vertices. Both effects are thus mechanistically linked to the cold-denaturation of the normal DNA origami triangles.

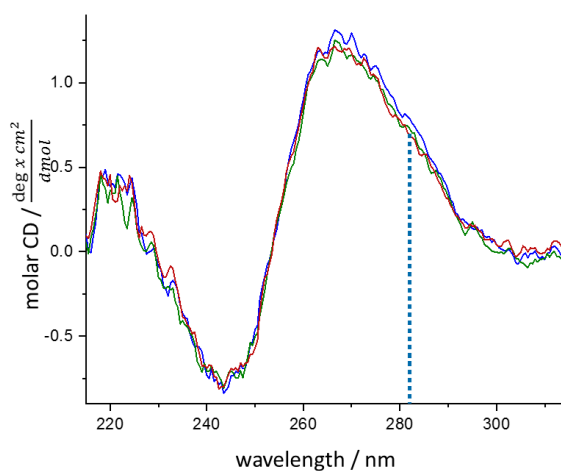


Figure S8: CD spectra of the dsDNA M13mp18 scaffold at 5 °C, 21 °C, and 37 °C (blue, green, and red, respectively) in 4 M GdmCl.

7. Additional AFM images of “cut triangles” and statistics of temperature-dependent damages

Table S2: Individual counts of “cut triangles” without GdmCl at RT (reference) and in the presence of 4 M GdmCl at 5 °C and 20 °C.

$N_{(\text{image})}$	T / °C	intact / %	broken trapezoids / %	collapsed triangles / %	dissociated vertices / %	$N_{(\text{origami})}$
4	RT	91.32 ±1.69	3.23 ±4.33	1.49 ±1.09	3.97 ±2.80	403
6	20	62.43 ±2.69	12.70 ±3.57	7.22 ±2.00	17.65 ±1.79	748
6	5	64.59 ±6.28	14.25 ±3.98	2.70 ±0.76	18.46 ±3.01	1446

The temperature insensitivity of the chirality of the relaxed dsDNA scaffold and the lack of cold-denaturation at the vertices in the “cut triangles” convincingly evidence that suprastructural strain transmitted from trapezoids to the vertices drives the cold-denaturation of the latter.

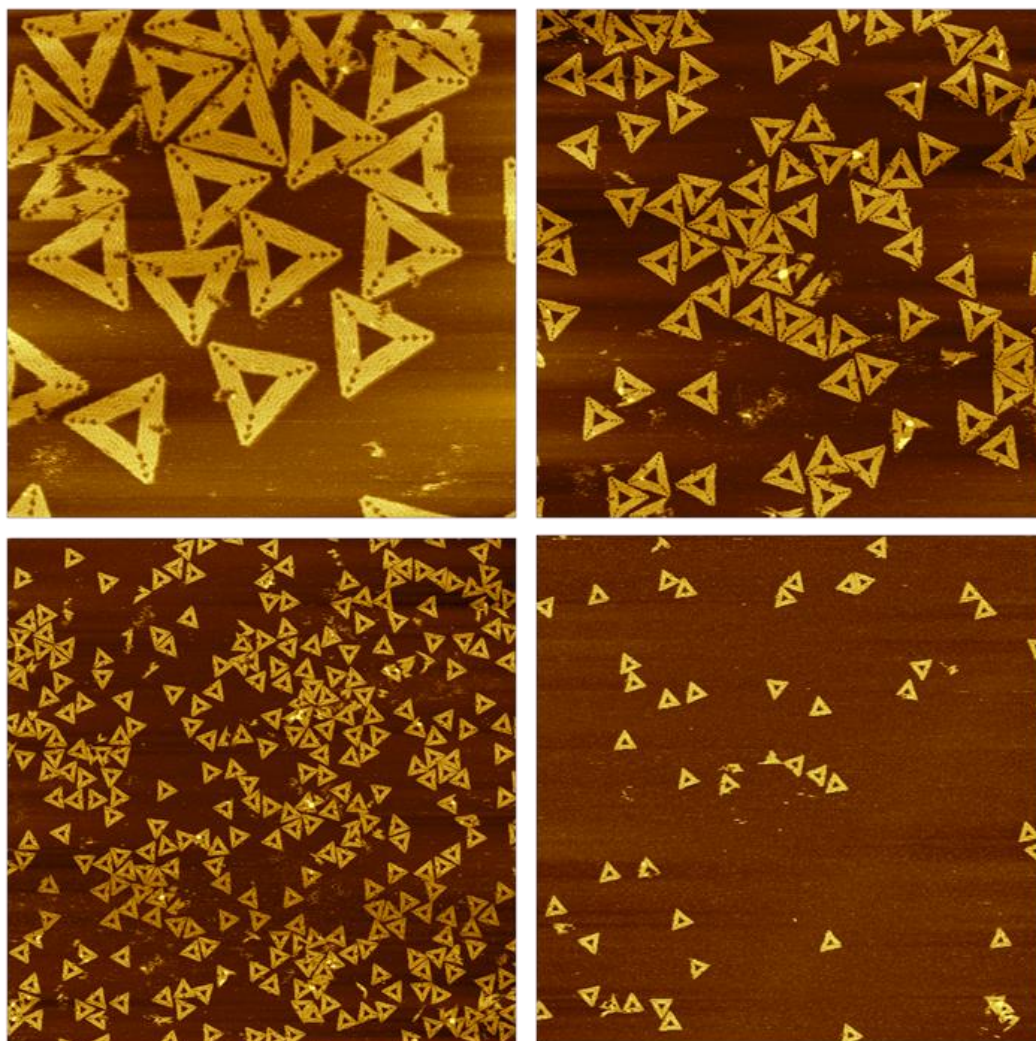


Figure S9: Additional AFM images (top left 0.6 x 0.6 μm^2 , top right 1.5 x 1.5 μm^2 , bottom right and left 3 x 3 μm^2) of cut DNA origami triangles after incubation at RT and without GdmCl, measured in liquid. Height scales are 5.0 nm.

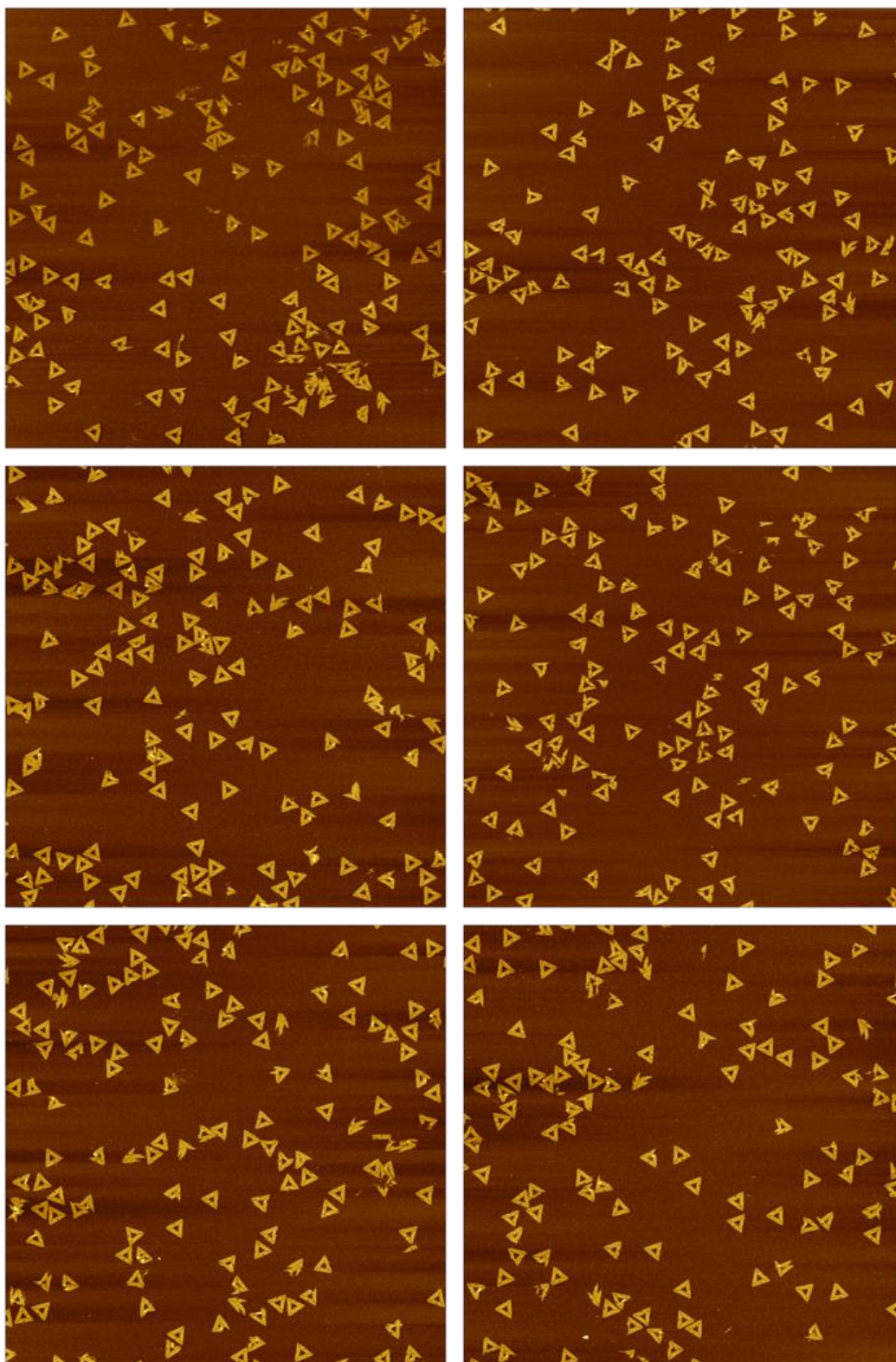


Figure S10: Additional AFM images ($3 \times 3 \mu\text{m}^2$) of cut DNA origami triangles after incubation at 20°C and with 4 M GdmCl, measured in liquid. Height scales are 5.0 nm.

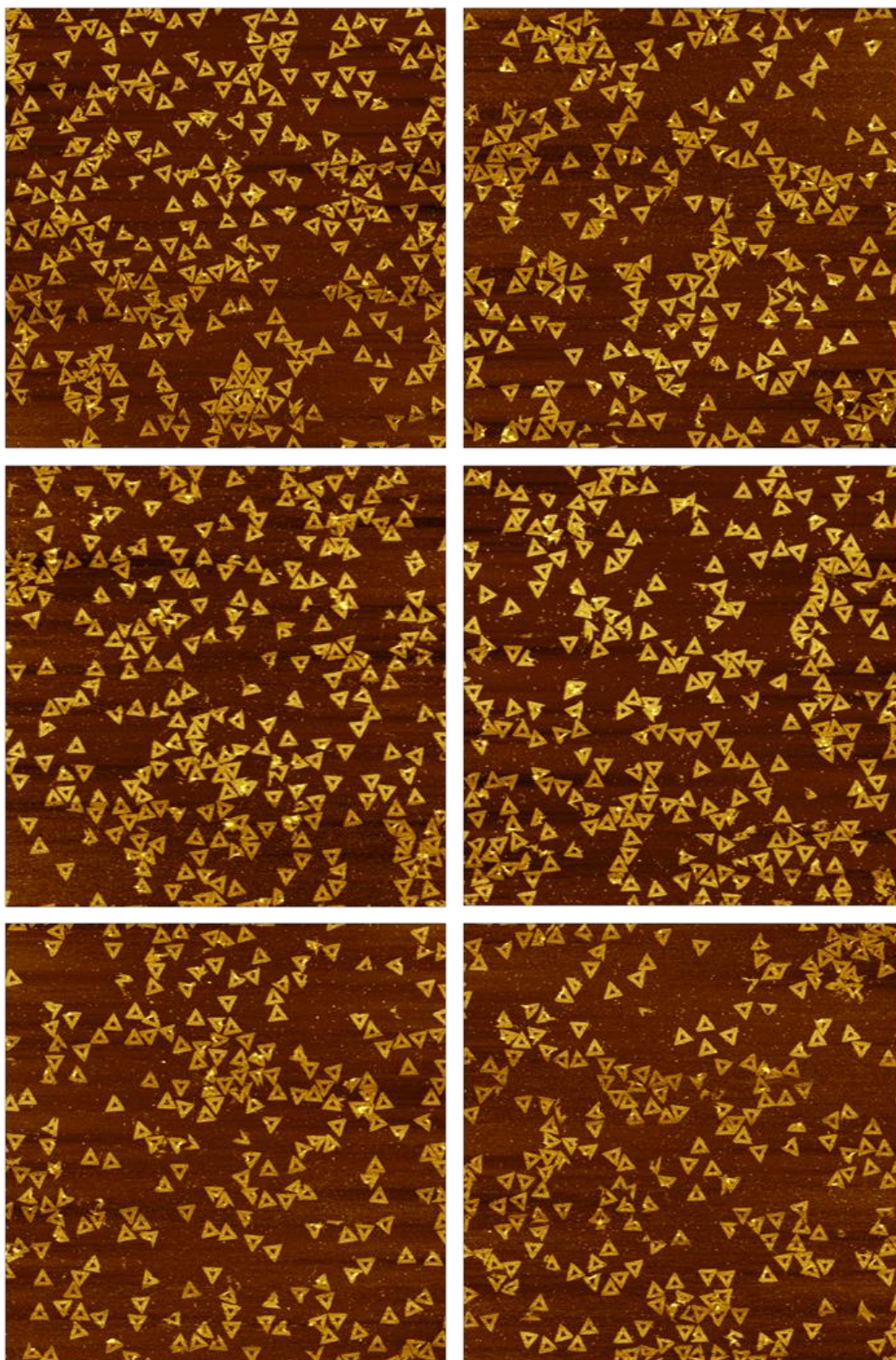


Figure S11: Additional AFM images ($3 \times 3 \mu\text{m}^2$) of cut DNA origami triangles after incubation at 5°C and with 4 M GdmCl, measured in liquid. Height scales are 5.0 nm.

1. P. W. K. Rothmund, *Nature*, 2006, **440**, 297-302.
2. A. Rossberg, T. Reich and G. Bernhard, *Anal Bioanal Chem*, 2003, **376**, 631-638.
3. H. F. Kaiser, *Psychometrika*, 1958, **23**, 187-200.